International Journal of General Engineering and Technology (IJGET)
ISSN 2278-9928
Vol. 2, Issue 2, May 2013, 29-38

International Academy of Science, Engineering and Technology
Connecting Researchers; Nurturing Innovations

IONIC LIQUIDS CLASSIFICATION FOR FUEL DESULPHURIZATION

SYAMSUL B. ABDULLAH[1], Z. MAN[2], L. ISMAIL[2], A. MAULUD[2] & M. A. BUSTAM[2]

[1]Faculty of Chemical and Natural Resources Engineering, Universiti Malaysia Pahang, Lebuhraya Tun Razak, 26300 Gambang, Pahang, Malaysia

[2]PETRONAS Ionic Liquid Centre, Chemical Engineering Department, Universiti Teknologi PETRONAS, Bandar Seri Iskandar, 31750 Tronoh, Perak, Malaysia

ABSTRACT

An analysis was applied to 35 types of ionic liquids (ILs) where three basic physical properties have been considered in predicting their relationships with fuel desulphurization performance. By mapping the original data of density versus molecular weight, it provided a quick indication of some form of relationship between these two variables based on the chemical structure of the anion in the classified ionic liquids, especially in sulphate, phosphate and cyano-based ILs. The mapping provided a quick and simple approach in estimating the potential of the ionic liquids' performance for fuel desulphurization. Conceivably influenced from these three basic physical properties, a modest and fairly good correlation was derived through statistical approach.

KEYWORDS: Ionic Liquids, Desulphurization, Density, Molecular Weight, Data Mapping

INTRODUCTION

Sulphur content in fuel has become a major environmental issue worldwide. Since June of 2006, the regulations in the US have required a reduction of sulphur in transport fuel from 500 to 15 ppm [1-3]. Meanwhile, in Europe, the regulation on sulphur in transport fuel required it to be less than 10 ppm by 2010 [4-5]. Until now, desulphurization can only be obtained via the heterogeneous catalytic hydrodesulfurization (HDS) process in petroleum plants. The main drawbacks of the HDS process include high operating temperature of 300˚C or above, high H_2 pressure of up to 4MPa, high energy costs and difficulty in removing aromatic heterocyclic sulphur compounds such as benzothiophene (BT) and its derivatives [6]. Therefore, ionic liquids (ILs) may be potential candidates in overcoming HDS' drawbacks in removing aromatic heterocyclic sulphur compound.

These days, research in ILs is attracting more attention as compared to traditional organic solvents, which could be due to these negligible vapour pressure, non-flammability and thermally stable kind of substances [7-9]. One of the most appealing features of using ILs is their potential to be custom-made with pre-selected characteristics (e.g. moisture stability, density, viscosity and miscibility with other co-solvents) through careful selection of the cation, anion or both [9]. Due to the large number of possible ILs via various cation and anion combinations, it is often impractical to use trial and error methods to find a suitable IL for a given task [11, 15]. Based on the increasing amounts of physical property data generated by researchers, there is a great need to introduce an easier method of recognizing possible relationships between the physical properties data for a series of ILs using data mapping for preliminary screening of ILs for desulphurization purposes.

In the present study, three physical properties of 35 types of ILs have been highlighted to gain more insight into developing a quicker screening method for the desulphurization process. By manipulating the data and using statistical

approach, a comparison and explanation for the similarities and grouping between the physical properties of the ILs in the plotted data could help predict the desulphurization performance for a new emerging ILs.

MATERIAL AND METHOD

Some of the ILs investigated in this work was synthesized in-house based on a published method [12] while some were purchased from Merck with stated halide content of less than 1%. For in-house synthesized ILs, the halide content was determined by ion chromatography (850 Professional IC, Metrohm, Switzerland), and the results were collected using MagIC Net 2.1 software. Meanwhile, the water content of the ILs was determined using coulometric Karl Fisher autotitrator, Mettler Toledo DL39 with CombiCoulomat fritless Karl Fisher reagent (Merck). Both halide and water content measurements were done in triplicate and the average value is considered. Table 1 shows the list of all investigated ILs in this study. The molecular weight of each ILs was appropriately taken from COSMOtherm software. The densities of the ILs were measured using a rotational automated density meter, Anton Paar DMA 5000M, based on published procedures [13], and the results obtained in this research are in agreement with previously published data, available via ILTHERMO database website.

Refractive index (RI) of the ILs was determined with an ATAGO RX-5000 Alpha digital refractometer at constant temperature to within ± 0.1°C. The instrument was calibrated by measuring the refractive index of deionized water. The sample support was rinsed with acetone and dried with a paper towel [13]. All the measurements were done in triplicate and the average value was used for this study.

In the present extractive desulphurization process, a mixture of *n*-dodecane and benzothiophene (1000µg/mL) was used as model fuel. The extraction was carried out in 25mL screw-cap vials. The mixture of equal mass ratio between ILs and model fuel was vigorously stirred at room temperature for 30 min and another 30 min was needed for settling to attain equilibrium. The ILs has higher density than the model fuel. The upper phase which was the model fuel could be withdrawn easily and analyzed for its sulphur content using HPLC (DAD detector, reverser-phase Zorbax SB-C18 column). Based on the values obtained, the material balance was prepared. At equilibrium, the sulphur partition coefficient determines the extent of the mobility of sulphur into ILs phase. The sulphur partition coefficient is defined as the ratio of equilibrium concentration of sulphur in ILs phase (S_a) to that in model fuel phase (S_b), as shown in equation 1 below. The details about the procedures and analysis are provided elsewhere [14].

$$K_d = \frac{S_a}{S_b} \tag{1}$$

The statistical analysis and correlation were performed by utilizing the MATLAB software package. The original data was analyzed by auto-scaling it, particularly by subtracting column averages and dividing it by the column standard deviations which applied as data normalization. This way, each of the variables (namely molecular weight, density and refractive index) was given identical load in identifying the linear correlation using a statistical approach.

RESULTS AND DISCUSSIONS

The aim of this paper is to show that the plot of the original density data (ρ) against the molecular weight (MW) can provide a quick indication of the relationship between the variables if the classification of the data is done correctly. In addition, the plot would easily show any outliers or other aberrations among the data. In this study, the original data was plotted as shown in Figure 1 and the variables used in constructing it were tabulated as shown in Table 2. For easy pattern justification of the data plot, the data has been categorized into two groups depending on their sulphur partition coefficient

(K_d). Desulphurization performance can be identified from the K_d value; i) $K_d > 1$ indicates that the sulphur removal is more than 50% from model fuel and ii) $K_d < 1$ indicates that the removal is less than 50%. This value has become an important benchmark in this study as the basic selection criteria for categorizing ILs.

Figure 1 presents the plotted data which shows scatterings of all types of ILs within the studied range as the desulphurization process was carried out. This leads to the observation that all 35 types of ILs showed no discernible pattern for separation purposes in terms of the desulphurization performance. On the other hand, when the same data were categorized based on the chemical structure of the ILs anion and re-plotted, clear separation regions can be observed, as shown in Figure 2. The four classifications identified in this figure are cyano-based ILs (correlation line with $R^2 = 0.9102$), phosphate-based ILs (correlation line with $R^2 = 0.9893$), sulphate-based ILs (correlation line with $R^2 = 0.933$) and others, including [C_4mim][BF_4], [C_4mim][PF_6], [C_4mim][FAP], [C_2mim][SCL] and [C_2mim][TOS] which cannot be grouped. Meanwhile, the sulphate-based ILs formed a stringent line on the ρ against MW plot. By excluding [P_{5551}][MSO_4], all the sulphate-based ILs with $K_d > 1$ seemed to reside on the top-left region while the sulphate-based ILs with $K_d < 1$ resided on the opposite region. For [P_{5551}][MSO_4], its exception might probably be due to its cation charge which is not situated on the aromatic site of this ILs. For further analysis, the classifications of individual ILs will be discussed in details after the data have been normalized.

The cyano-based ILs consisted of 1-butyl-3-methylimidazolium thiocyanate ([C_4mim SCN]), 1-butyl-3-methylimidazolium dicyanamide ([C_4mim DCA]) and 1-butyl-3-methylimidazolium tricyanomethane ([C_4mim TCM]) where their chemical structures are presented in Figure 3. Referring to the experimental results of the extractive desulphurization performance (refer Table 2), it shows that K_d value increases with increasing number of cyano group (−C≡N) uptick on the anion structures and the order was as follows; SCN < DCA < TCM. Figure 4 shows the normalized data of ρ against MW plot. There is a strong linear correlation between the ρ and MW with a correlation coefficient, R^2 of greater than 0.9. By comparing the linear correlation line and the desulphurization performance of cyano-based ILs, a similar trend is apparent where TCM can be found at the top spot of the correlation followed by DCA and SCN, as shown in Figure 4. The great thing about this similarity is that it could possibly become the predictive mapping for a new generation of IL that consists of cyano group, to be used purposely for fuel desulphurization, just by plotting ρ against MW.

The second classified group was phosphate-based ILs which consisted of three compounds, namely 1-butyl-3-methylimidazolium dihydrogenphosphate ([C_4mim DHP]), 1-butyl-3-methylimidazolium dimethylphosphate ([C_4mim DMP]) and 1-butyl-3-methylimidazolium dibutylphosphate ([C_4mim DBP]). Figure 5 depicts their chemical structures and the experimental results from the desulphurization performance revealed that K_d value decreases as the number of alkyl chain lost on both the cation and anion parts, which follows the order of DBP > DMP > DHP. It can be explained that by losing the alkyl chain, the coulombic attraction between the cation and the anion of the ILs became stronger, thus hindering the sulphur compound's interaction with the ILs. Figure 6 depicts the normalized data of ρ against MW plot. It can be seen that there is a strong linear correlation between ρ and MW with correlation coefficient, R^2 value of 0.99. It seems obvious that the linear correlation of phosphate-based ILs followed the same order of desulphurization performance trend. Through this mapping, it could become one of the simplified methods in the search for a new phosphate-based IL for fuel desulphurization.

It was observed that the ILs in the classified groups had interacted in a parallel behaviour (having characteristics in common), as apparent by the patterns seen on the groups' plotted data. Upon inspection, the largest classified group which was the sulphate-based ILs had also shown a linear correlation, as seen in Figure 7. The plot depicts on the upper

side of the linear correlation, as represented by filled-dots, are the ILs with K_d values greater than 1 while on the lower side, depicted by unfilled-dots, are the ILs with K_d values of less than 1. A parallel behaviour can be observed in Figures 4, 6 and 7 where each group showed that the best ILs in their group are plotted at the top of their correlation. By introducing these three mappings, they may demonstrate an easier method to the researchers, for identifying the potential of their latest synthesized ILs towards desulphurizing fuel especially with regards of the petroleum industry.

Evidently, in order to study the linear correlation of sulphate-based ILs with the studied variables, a statistical approach was completed and the result is presented in Table 3. K_d is the actual value while MW, ρ and RI with mean values of 251.2560, 1.2404, 1.4782 and standard deviation of 50.1583, 0.1156, 0.0151, respectively, were later normalized to obtain the value of zero for mean and one for standard deviation of each studied variable. The RI variable seemed to have some minor effect on the K_d values, with only 8.77% of the data fitted the proposed linear correlation, according to the R^2 value. Meanwhile, for single data of ρ and MW, the calculated R^2 values were 0.8459 and 0.8596, respectively. Indeed, the corresponding correlation was fairly good in determining K_d value. Furthermore, it should be mentioned that the generated linear correlation with the combined variables showed improvement, by looking at the R^2 value which changed from 0.8683 to 0.8717. Other scattered data which could not be classified accordingly, neither on the original nor on the normalized plot, remained unexplained.

CONCLUSIONS

A mapping of density (ρ) against the molecular weight (MW) with appropriate classification provides a quick and simple approach in estimating the potential of ILs performance for fuel desulphurization. The three identified groups were cyano-based, phosphate-based and sulphate-based ILs. A simple and fairly good correlation with three studied variables, a priori expected to influence, was successfully derived through statistical approach.

REFERENCES

1. Bosmann, A., Datsevich, L., Jess, A., Lauter, A., Schmitz, C., Wasserceid, P. (2001). **Chemical Communications**, 2494-5
2. Zhao, D., Sun, Z., Li, F., Shan, H., (2009). **Journal of Fuel Chemistry and Technology**, Vol. 37, pp. 194-198
3. Liu, D., Gui, J., Song, L., Zhang, X., Sun, Z. (2008). **Petroleum Science & Technology**, Vol. 26, pp. 973-982
4. Alonso, L., Arce, A., Francisco, M., Soto, A. (2008). **Fluid Phase Equilibria**, Vol. 270, pp. 97-102
5. Wilfred, C.D., Chong, F.K., Man, Z., Bustam, M.A., Abdul Mutalib, M.I., Chan, Z.P. (2012). **Fuel Processing Technology**, Vol. 93, 85-9
6. Gao, H., Luo, M., Xing, J., Wu, Y., Li, Y., Li, W., Liu, Q., Liu, H. (2008). **Industrial & Engineering Chemistry Research**, Vol. 47, pp. 8384-8
7. Marsh, K.N., Boxall, J.A., Lichtenthaler, R. (2004). **Fluid Phase Equilibria**, Vol. 219, pp. 93-8
8. Arce, A., Earle, M.J., Katdare, S.P., Rodriguez, H., Seddon, K.R. (2006). **Chemical Communication**, Vol. , pp. 2548-50
9. Arce, A., Earle, M.J., Katdare, S.P., Rodriguez, H., Seddon, K.R. (2007). **Fluid Phase Equilibria**, Vol. 261, 427-33

10. Holbrey, J.D., Martin, I.L., Rothenberg, G., Seddon, K.R., Silvero, G., Zheng, X. (2008). **Green Chemistry**, Vol. 10, pp. 87-92

11. Heintz, A. (2005). **Journal of Chemical Thermodynamics**, Vol. 37, pp. 525-35

12. Holbrey, J.D., Reichert, W.M., Swatloski, R.P., Broker, G.A., Pitner, W.R., Seddon, K.R., Rogers, R.D. (2002). **Green Chemistry**, Vol. 4, 407-13

13. Yunus, N.M., Mutalib, M.I.A., Man, Z., Bustam, M.A., Murugesan, T. (2010). **Journal of Chemical Thermodynamics**, Vol. 42, pp. 491-5

14. Syamsul, A.B., Man, Z., Ismail, L., Maulud, A., Mutalib, M.I.A., Bustam, M.A. (2011). **Research Journal of Chemistry and Environment**, Vol. 15, 510-8

15. Parshad, H., Frydenvang, K., Liljefors, T., Larsen, C.S. (2002). **International Journal of Pharmaceutics**, Vol. 237, 193-207.

APPENDICES

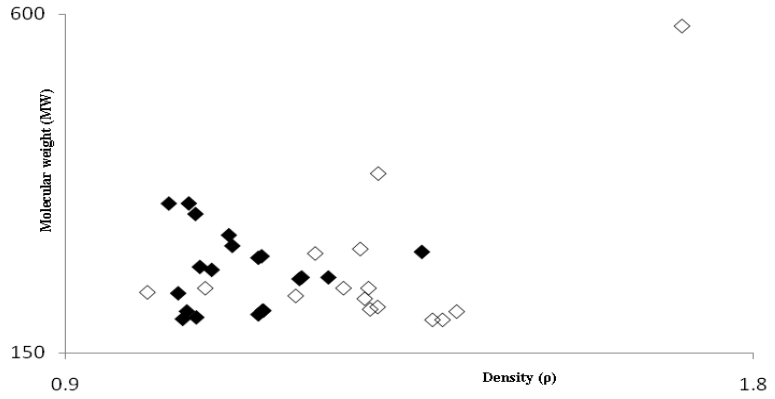

Figure 1: Graphical Presentation of the Original Data for 35 Types of ILs; Density (ρ) Against Molecular Weight (MW) where Filled-Dots Represent $K_d > 1$ While the Others Represent $K_d < 1$

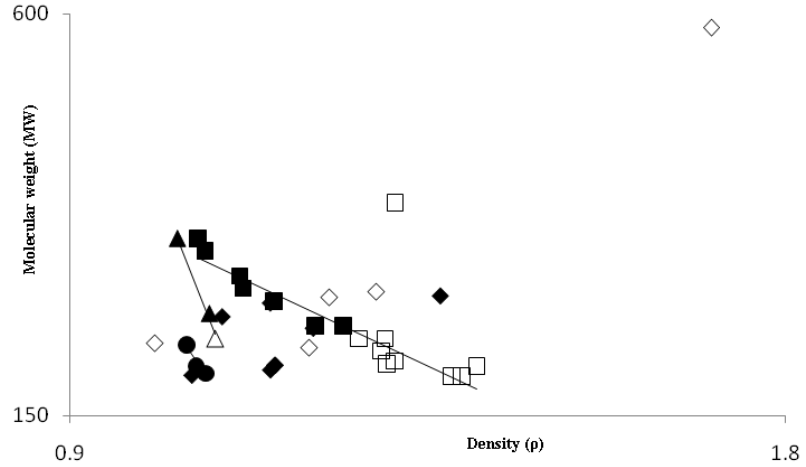

Figure 2: Graphical Presentation of the Original Data for 35 Types of ILs; Density (ρ) Against Molecular Weight (MW) with Identified Group; (Cyano-Based ILs, Circle-Plot; Phosphate-Based ILs, Triangle-Plot; Sulphate-Based ILs, Rectangular-Plot)

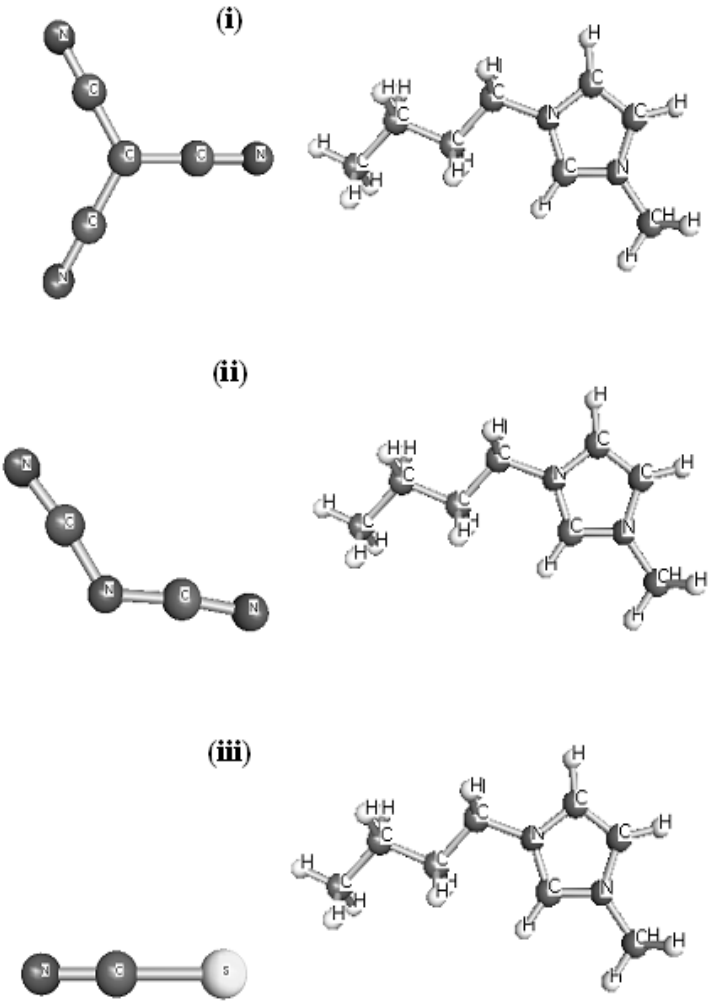

Figure 3: Chemical Structures of Cyano-Based ILs: (i) C_4mim TCM; (ii) C_4mim DCA and (iii) C_4mim SCN

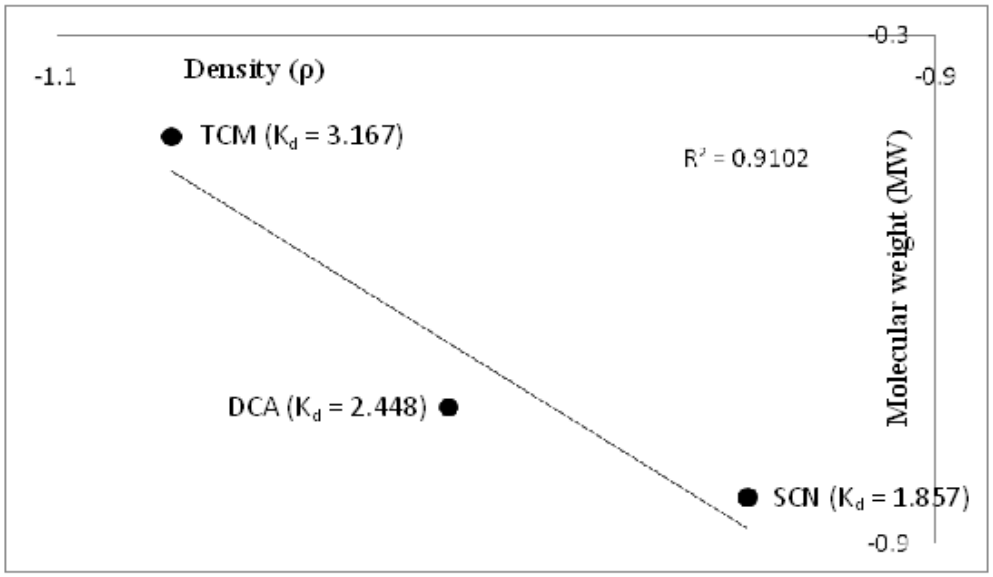

Figure 4: Standardized Data of Density (ρ) Plotted Against Molecular Weight (MW) of Cyano-Based ILs, $R^2 = 0.9102$

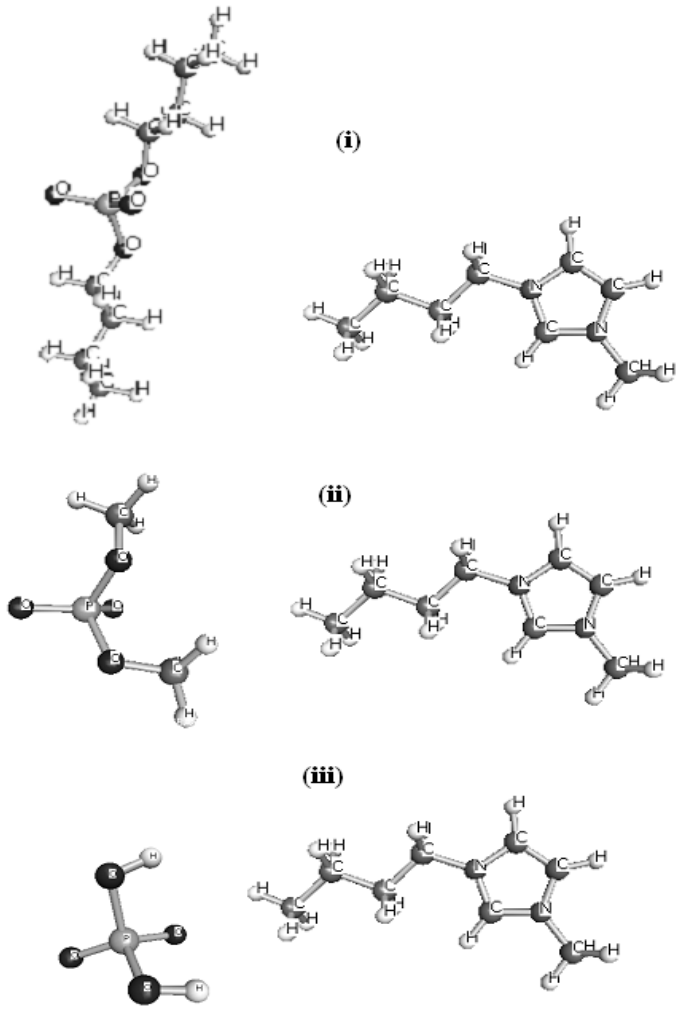

Figure 5: Chemical Structures of Phosphate-Based ILs: (i) C_4mim DBP; (ii) C_4mim DMP and (iii) C_4mim DHP

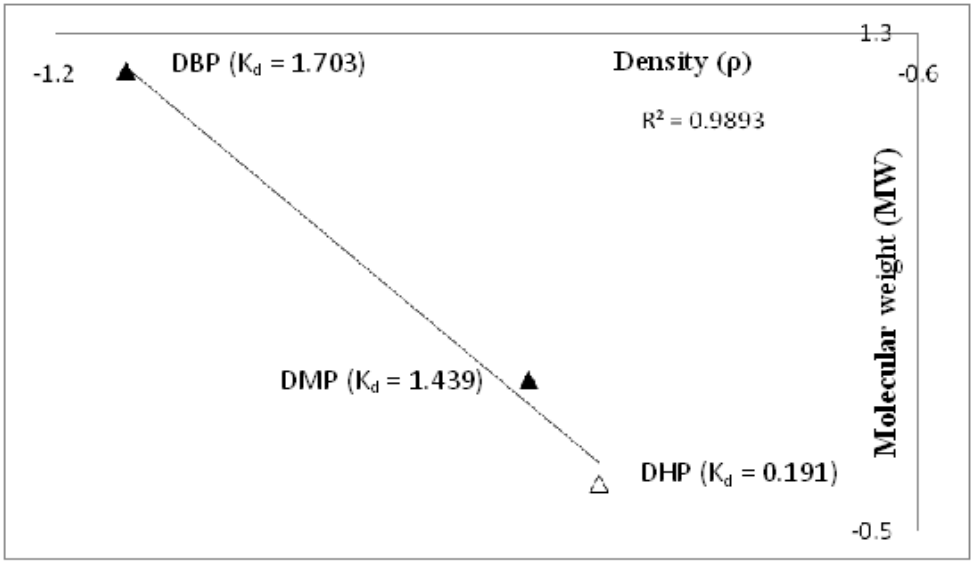

Figure 6: Standardized Data of Density (ρ) Plotted Against Molecular Weight (MW) of Phosphate-Based ILs, R^2 = 0.9893

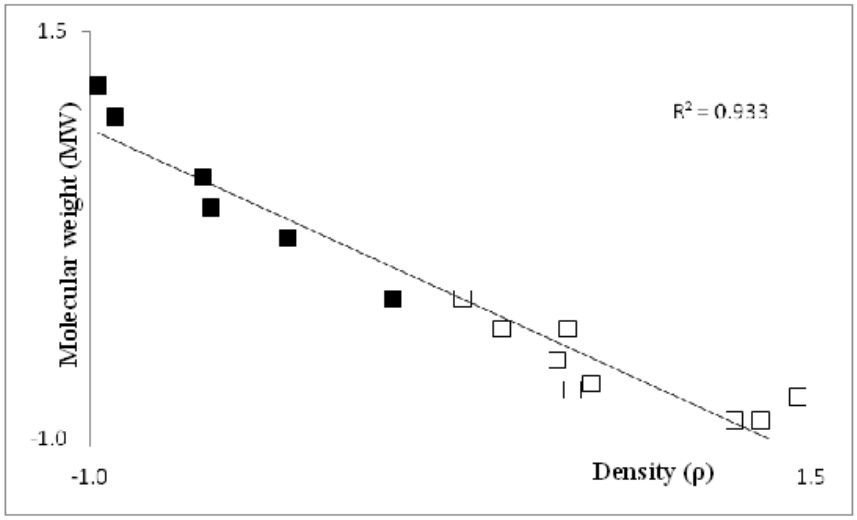

Figure 7: Standardized Data of Density (ρ) Plotted Against Molecular Weight (MW) of Sulphate-Based ILs, R^2 = 0.933, $[P_{5551}][MSO_4]$ was Excluded; (Filled-Dots Represent $K_d > 1$ While Others Represent $K_d < 1$)

Table 1: List of Investigated ILs in this Study

Acronym	Name of ILs
$P_{5\,5\,5\,1}$ MSO_4	Triphenylmethylphosphonium methylsulfate
C_1Py MSO_4	1-methylpyridinium methylsulfate
C_1Pyz MSO_4	1-methylpyrazolium methylsulfate
C_1im MSO_4	1-methylimidazolium methylsulfate
C_1mPyrr MSO_4	1,1-dimethylpyrrolidinium methylsulfate
C_2mim SCL	1-ethyl-3-methylimidazolium salicylate
C_2mim TOS	1-ethyl-3-methylimidazolium tosylate
C_4mim BF_4	1-butyl-3-methylimidazolium tetrafluoroborate
C_4mim PF_6	1-butyl-3-methylimidazolium hexafluorophosphate
C_4mim FAP	1-butyl-3-methylimidazolium tris(pentafluoroethyl)trifluorophosphate
C_4mim OTf	1-butyl-3-methylimidazolium trifluoromethanesulfonic
C_4mim Ac	1-butyl-3-methylimidazolium acetate
C_4mim NO_3	1-butyl-3-methylimidazolium nitrate
C_4mim DBP	1-butyl-3-methylimidazolium dibutylphosphate
C_4mim DMP	1-butyl-3-methylimidazolium dimethylphosphate
C_4mim DHP	1-butyl-3-methylimidazolium dihydrogenphosphate
C_4mim SCL	1-butyl-3-methylimidazolium salicylate
C_4mim SCN	1-butyl-3-methylimidazolium thiocyanate
C_4mim TCM	1-butyl-3-methylimidazolium tricyanomethane
C_4mim DCA	1-butyl-3-methylimidazolium dicyanamide
C_4mim Imd	1-butyl-3-methylimidazolium imidazolide
C_4mim Pyd	1-butyl-3-methylimidazolium pyrazolide
C_4mim BZT	1-butyl-3-methylimidazolium benzoate
C_4mim HSO_4	1-butyl-3-methylimidazolium hydrogensulfate
C_4mim OSO_4	1-butyl-3-methylimidazolium octylsulfate
C_1mim MSO_4	1,3-dimethylimidazolium methylsulfate
C_2mim MSO_4	1-ethyl-3-methylimidazolium methylsulfate
C_4mim MSO_4	1-butyl-3-methylimidazolium methylsulfate
C_1eim ESO_4	1-methyl-3-ethylimidazolium ethylsulfate
C_2eim ESO_4	1,3-dethylimidazolium ethylsulfate
C_4eim ESO_4	1-butyl-3-ethylimidazolium ethylsulfate
C_1bim BSO_4	1-methyl-3-butylimidazolium butylsulfate
C_2bim BSO_4	1-ethyl-3-butylimidazolium butylsulfate
C_4bim BSO_4	1,3-dibutylimidazolium butylsulfate
C_8mim Cl	1-octyl-3-methylimidazolium chloride

Table 2: Database of Molecular Weight (MW), Density (ρ) and Refractive Index (RI) of Studied Ionic Liquids

Name of ILs	MW	ρ	RI	K_d
$P_{5\,5\,5\,1}$ MSO_4	388.42	1.3086	1.5607	0.370
C_1Py MSO_4	205.23	1.4113	1.5213	0.234
C_1Pyz MSO_4	194.21	1.3927	1.4688	0.266
C_1im MSO_4	194.21	1.3796	1.4822	0.298
C_1mPyrr MSO_4	211.28	1.3078	1.4487	0.316
C_2mim SCL	248.28	1.2051	1.5612	1.020
C_2mim TOS	282.36	1.2261	1.5407 (*1.5380*)*	0.471
C_4mim BF_4	226.02	1.2006	1.4238 (*1.4215*)*	0.960
C_4mim PF_6	284.19	1.3652	1.4110 (*1.4084*)*	1.083
C_4mim FAP	584.23	1.7061	1.3772	0.923
C_4mim OTf	288.29	1.2851	1.4380 (*1.4368*)*	0.942
C_4mim Ac	195.24	1.0527	1.4740	1.564
C_4mim NO_3	201.22	1.1516 (*1.1565*)*	1.5059	1.500
C_4mim DBP	348.42	1.0346	1.4534	1.703
C_4mim DMP	264.26	1.0751	1.4790	1.439
C_4mim DHP	236.21	1.0822	1.5031	0.191
C_4mim SCL	276.33	1.1515	1.5367	1.632
C_4mim SCN	197.31	1.0704	1.5335	1.857
C_4mim TCM	229.28	1.0467	1.5081	3.167
C_4mim DCA	205.26	1.0581 (*1.0580*)*	1.5064	2.448
C_4mim Imd	206.29	1.1580	1.5151	1.857
C_4mim Pyd	206.29	1.1571	1.5255	1.703
C_4mim BZT	260.33	1.0905	1.5224	2.030
C_4mim HSO_4	236.29	1.2958	1.4907	0.205
C_4mim OSO_4	348.51	1.0606 (*1.0601*)*	1.4686 (*1.4699*)*	2.030
C_1mim MSO_4	208.24	1.2980	1.4834 (*1.4827*)*	0.409
C_2mim MSO_4	222.26	1.2909	1.4772	0.493
C_4mim MSO_4	250.32	1.2082 (*1.2124*)*	1.4755 (*1.4778*)*	1.222
C_1eim ESO_4	236.29	1.2631	1.4791 (*1.4794*)*	0.587
C_2eim ESO_4	250.32	1.2431	1.4741	0.7544
C_4eim ESO_4	278.38	1.1557	1.4714	1.273
C_1bim BSO_4	292.40	1.1173	1.4801	1.063
C_2bim BSO_4	306.42	1.1130	1.4787	1.196
C_4bim BSO_4	334.48	1.0693	1.4735	1.439
C_8mim Cl	230.78	1.0065	1.5087 (*1.5050*)	0.887

()* - open source available from ILTHERMO database website

Table 3: The Simplified Analysis of Variance (ANOVA) with Proposed Linear Correlation

Equation	R^2	P Value
K_d = -0.1638[RI] + 0.7857	0.0877	0.2840
K_d = -0.5089[ρ] + 0.7857	0.8459	0.0
K_d = 0.513[MW] + 0.7857	0.8596	0.0
K_d = -0.1994[ρ] + 0.3204[MW] + 0.7857	0.8683	0.0
K_d = -0.1223[ρ] + 0.3866[MW] – 0.0389[RI] + 0.7857	0.8717	0.0

P value – the value should less than 0.05 in order to justify the proposed correlation to be statistically significant